



Surface growth by random deposition of rigid and wetting clusters



D.A. Mirabella, C.M. Aldao

Institute of Materials Science and Technology (INTEMA), University of Mar del Plata and National Research Council (CONICET), Juan B. Justo 4302, Mar del Plata B7608FDQ, Argentina

ARTICLE INFO

Available online 24 September 2015

Keywords:

Surface growth
Dynamic scaling
Cluster deposition
Monte Carlo simulations

ABSTRACT

Surface grown by the deposition of rigid and wetting clusters has been investigated using Monte Carlo simulations in $1 + 1$ dimensions. Dynamic scaling exponents were determined using the time evolution of the roughness, the local width, the height–height correlation function, and the power spectrum. The values obtained for the roughness exponent clearly reflect the growth mechanism adopted for deposition. In the case of wetting clusters, the roughness exponent corresponds to that of random deposition, but a correlation appears for low window size, with a crossover that is related to the average cluster size and cluster size distribution. On the other hand, rigid cluster deposition belongs to the KPZ universality class. However, determined scaling exponents converge very slowly to those corresponding to KPZ.

© 2015 Elsevier B.V. All rights reserved.

1. Introduction

The kinetic roughening of thin-film growth fronts under non-equilibrium conditions has attracted considerable interest due to their wide application in critical components for electronic, magnetic, and optical devices [1]. The functionality of these films is determined by their physical structure, in particular the surface roughness and the grain size distribution in the case of polycrystalline films. A complete characterization of the surface and the microstructure can provide a deeper understanding of the processes that drive the physical evolution during film formation. In many cases, the dynamics of the growing film leads to spread correlations over the whole system and produce scale invariant surfaces that are described by the Family–Vicsek ansatz [2–5]. Depending on the growing mechanisms, the resulting surface evolution can be determined as belonging to distinct universality classes. Thus, measuring the set of scaling exponents for a particular system allows to associate it with some universality class and consequently with a dominant growing mechanism.

Random deposition of agglomerated particles (clusters) is one of the commonly used methods in the fabrication of nanostructured materials. Since clusters at the surface occupy more than one unit size, depending on the deposition mechanisms, a porous bulk can be generated. This property is desirable in manufacturing nanostructured materials for many applications, such as magnetic storage and solar cells [6,7]. In the past, a lot of work has been devoted to study the deposition of particles. However, less attention has been paid to the cluster incorporation process, but at least two different universality classes were reported [8–10].

In the present work, we report a dynamic scaling analysis of a surface formed by deposition of clusters onto a one-dimensional substrate. We studied two types of cluster incorporation mechanisms, one in which the clusters fall randomly and wet the surface copying its profile,

and the resulting aggregate is not porous. Hereafter, we will refer to this model as wetting cluster deposition (WCD). The second model deals with rigid clusters that stick at the first point of contact and do not change their shape after their incorporation to the substrate, generating a porous deposit. Hereafter, we will refer to this model as rigid cluster deposition (RCD). We also studied the effects of the cluster size distribution on the scaling exponents.

Hellmut Haberland and co-workers have investigated the structure of thin films grown by energetic cluster impact deposition [11]. In this technique, ionized metal clusters are electrically accelerated onto the substrate. It has been observed that the final film morphology depends on the deposition parameters, such as the size and the incident energy of the clusters. In particular, the increase of the cluster impact energy leads to the formation of more compact films. They found a transition from a porous film with multiple voids to a dense film with a nearly bulk density as the incident energy is increased from 0.1 eV/atom to 10 eV/atom [12]. For low kinetic energies, clusters stick at the first point of contact, resembling a ballistic deposition. For high-impact energies, incident clusters lead to a redistribution of atoms in which the substrate atoms are involved, a smoother resulting surface, and then the Edwards–Wilkinson class is expected. At intermediate energies, impinging clusters wet the surface without affecting the substrate atoms, as seen in Ref. [12] for Mo clusters. In this case, we expect that this technique resembles the WCD. Softer metals are prone to wet the surface after landing. Indeed, in Refs. [13] and [14] it can be seen that Al and Cu clusters with very low kinetic energy incorporate to the surface without the generation of voids and no intermixing resembling the WCD.

To obtain the scaling exponents for the rigid cluster deposition (RCD), we calculated the interface width, $W(L,t)$ and also the local width (LW), the height–height correlation function (HHCF), and the power spectrum (PS). The local surface roughness $w(l,t)$, which

represents height fluctuations in different length scales, shows a cross-over related to the cluster lateral size, giving rise to a small-scale roughness exponent that differs from the global one [15,16]. Also, for distances smaller than the mean cluster size, we found different values for the roughness exponents, obtained from HHCF and LW, whereas for large distances, the exponents have the same values and are determined by the growth mechanism adopted for deposition, as reported in Refs. 9 and 10. For rigid clusters, the scaling exponents converge very slowly to those of KPZ universality class for very large system sizes [8], whereas for wetting cluster deposition (WCD), the scaling exponents correspond to those of random deposition but a correlation appears at small scale due to cluster finite size.

2. Dynamic scaling framework

The most obvious quantitative characteristic of a rough surface is the root-mean square of the height field, known as the surface width or roughness

$$W(L, t) = \sqrt{\frac{1}{L} \sum_{i=1}^L [h(i, t) - \bar{h}(t)]^2}, \tag{1}$$

where $h(i, t)$ is the surface height measured from the flat substrate of size L at the position i at the time t , and $\bar{h}(t)$ is the mean height of the interface at the same time.

Family and Vicsek proposed a scaling relation that connects the surface roughness with the linear size of the lattice and time [3]. This scaling relation, applicable to a large number of growth models, is written as

$$W(L, t) \sim L^\alpha f(t/L^z), \tag{2}$$

where the scaling function $f(u)$ is a function that behaves as u^β for $u \ll 1$ and as a constant for $u \gg 1$. The parameters α and β are the roughness and growth exponents, respectively, and $z = \alpha/\beta$ is the dynamic scaling exponent. α and β constitute a pair of numbers that can be used to classify quantitatively the spatial and temporal scaling of growing surfaces and then to identify the growth process.

On the other hand, quantitative information about the height fluctuations and lateral correlation is given by the height–height correlation function HHCF

$$C(l, t) = \langle (h(x+l, t) - h(x, t))^2 \rangle^{1/2}. \tag{3}$$

$C(l)$ constitutes a quantitative description of how the heights at different points of the surface are correlated as a function of their separation. For a self-affine surface, $C(l, t)$ scales with l as

$$C(l, t) \approx l^\alpha f(t/l^z), \tag{4}$$

Another important quantity to characterize the surface growing process is the local interface width $w(l, t)$ defined as

$$w(l, t) = \left\langle \frac{1}{l} \left(h^2(x, t) - \langle h(x, t) \rangle \right)^2 \right\rangle^{1/2}. \tag{5}$$

It is well known that $w(l, t)$ scales as

$$\begin{aligned} w(l, t) &\sim t^\beta, \text{ for } t \ll l^z, \text{ and} \\ w(l, t) &\sim t^\alpha, \text{ for } t \gg l^z, \end{aligned} \tag{6}$$

where l is the window size.

Finally, other convenient way of summarizing data is the spectral power density or structure factor

$$S(k, t) = \langle h(k, t)h(-k, t) \rangle, \tag{7}$$

being $h(k, t)$ the k th Fourier mode of the surface height deviation around its spatial average for a given time t

$$h(k, t) = \frac{1}{L^{1/2}} \sum_x [h(x, t) - \bar{h}(t)] \exp(ikx). \tag{8}$$

The structure factor scales as

$$S(k, t) = k^{-(2\alpha+1)} g(t/k^{-z}). \tag{9}$$

For $u \ll 1$ $g(u) = u(2\alpha + 1)/z$ and for $u \gg 1$ $g(u) = \text{constant}$, and then

$$\begin{aligned} S(k, t) &\sim k^{-(2\alpha+1)} \quad u \ll 1 \\ S(k, t) &\sim t^{(2\alpha+1)/z} \quad u \gg 1 \end{aligned} \tag{10}$$

Surface structures that preserve a similar morphology upon a change of magnification are termed self-affine and obey the well-known Family–Vicsek (FV) scaling ansatz, which plays a central role in growth theories [2–4]. However, not all systems exhibit FV scaling. For instance, it has been reported that the formation of features during etching or film growth by grains leads to a more complex roughening process [16,17]. On the other hand, an evolving pattern can show different scaling at the global and at the local length scales. Thus, a common set of scaling parameters is no longer adequate to characterize the dynamic behavior at different scales and additional exponents are needed to fully characterize the observed growth [18–21].

3. Monte Carlo modeling

We performed simulations using the standard Monte Carlo method in 1D. The surface is represented by a one-dimensional vector where each element corresponds to the height at each site. To study the dynamic scaling exponents, we used clusters of size $N \times N$ (a square) and $1 \times N$ (a horizontal rod). The deposition process starts building a cluster and choosing a site at random (i) over the surface. We evaluated two types of aggregation mechanisms. One in which the arriving cluster can disassemble, and it changes its shape by copying the surface profile. All sites between i and $i + N$ grow the cluster original height, and the growth is conservative (WCD model). The second model corresponds to rigid clusters in which they land atop of the highest surface site between i and $i + N$, giving rise to a non-conservative growth. If the site j , with $i \leq j \leq i + N$, presents the local highest site $h(j)$, then the cluster incorporation at the surface, for a horizontal rod, takes place changing the heights of all sites, from i to $i + N$ to $h(j) + 1$ (RCD model). A similar process is used for the deposition of a cluster of size $N \times N$ but finally the heights of all sites from i to $i + N$ are changed to $h(j) + N$. Other processes, such as rearrangement of surface particles (diffusion) or detachment, are not allowed.

Fig. 1 depicts the studied models. In the RCD model, once a cluster is in contact with a particle of the substrate, it is incorporated without changing its shape. In Fig. 1a, two clusters consisting of four particles, of 2×2 and 1×4 , are shown after arriving to the surface in their final position. Conversely, in the WCD model, arriving clusters are incorporated to the aggregate by wetting the surface. This means that the particles of the cluster can move down until making contact with a particle of the substrate. In Fig. 1b, the final aggregate morphology is depicted after the incorporation of two clusters as in Fig. 1a but using the rules of the WCD model.

The simulation starts from a flat substrate configuration and evolves with successive deposition of clusters until it approaches steady state. One Monte Carlo time corresponds to the deposition of one monolayer of particles. We checked that steady state was reached by assessing the evolution of the surface roughness. Monte Carlo simulations were

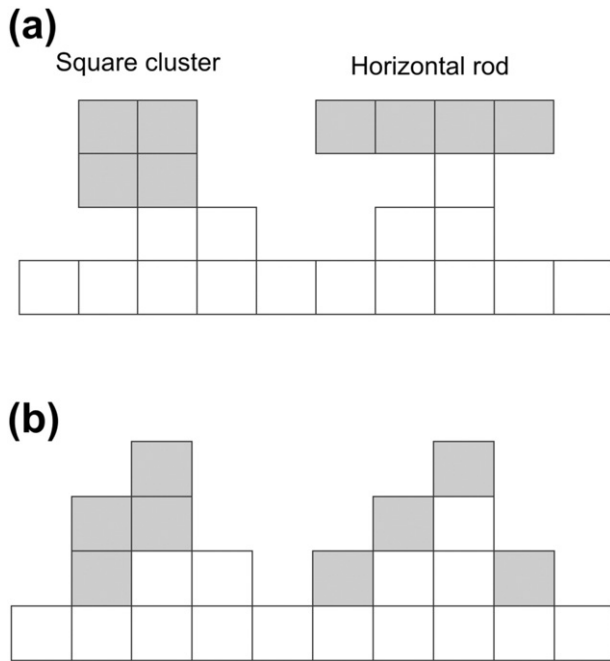


Fig. 1. Studied models. (a) Rigid cluster deposition model in which clusters are incorporated to the aggregate keeping their shape, as they make contact with the substrate. This type of deposition leads to a non-conservative growth as voids develop. (b) Wetting cluster deposition model in which every particle of the cluster can move down until making contact with the substrate.

carried out for systems of different lengths and periodic boundary conditions were used to avoid edge effects.

4. Results and discussion

Fig. 2 shows the HHCF and LW for the WCD model after the deposition of 1000 ML through clusters of size 1×10 on a substrate of $L = 2000$. As can be seen, both functions present a crossover that defines two regimes with different growth exponents, which is due to the cluster lateral size. For large window sizes, both functions have zero slope (uncorrelated), they are independent of l , as expected for a random deposition. At small scale the initial slopes are $\chi_1 = 0.5$ and

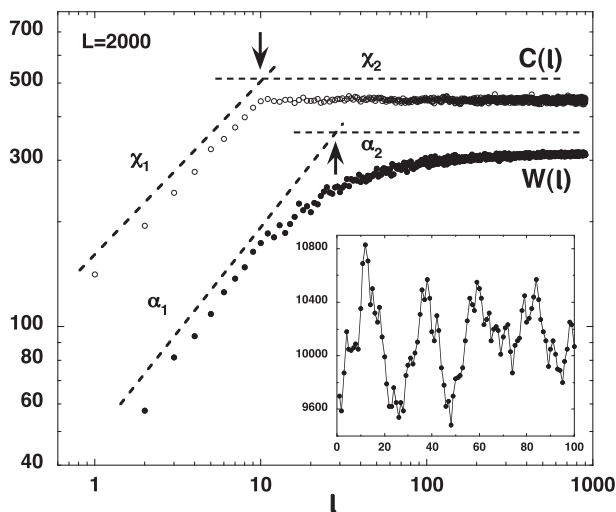


Fig. 2. Height–height correlation function and local roughness for the WCD model after the deposition of 1000 ML in rods of size $N = 10$ on a substrate of $L = 2000$. Crossovers are related to the rod size; the one corresponding to the HHCF matches it. The inset shows the resulting morphology that is correlated at short distances.

$\alpha_1 = 0.6$ for HHCF and LW, respectively. Interestingly, for the WCD model, this is not the result of a geometric effect of the grainy surface and the sliding window method, but due to the fact the surface sites under the cluster grow simultaneously [11]. Note that the crossover in the HHCF directly reflects the size of the clusters while for the LW the determined crossover is about 26, more than twice the cluster size.

The inset of Fig. 2 shows the resulting surface morphology (not in scale). As rods wet the surface, there is no trace of them at first sight. Interestingly, the HHCF and the LW show that close sites are correlated because the deposition is not random for distances smaller than the cluster size. In Ref. 15, a clustered surface is obtained by growing the film using a random deposition and then enlarging the size of each particle by a factor l . The resulting substrate ends up with a collection of terraces of size l . It is then obvious to see the correlation with a direct assess of the profile. Conversely, the resulting surface profile for the WCD does not seem to be correlated. However, the typical analysis used in growth dynamics reveals that we are dealing with a correlated surface. Interestingly, the local roughness exponent reported in Ref 15 $\alpha_1 = 1$ is not the same for the WCD $\alpha_1 \approx 0.6$.

Given the direct relation between the cluster size and the crossover in the HHCF, we studied the effect of having a mixture of clusters with two different sizes. In Fig. 3, we present the HHCF for the WCD model after the deposition of a mixture of rods of size 10 and 20. We define the parameter ρ , the ratio between the probability of depositing clusters of size 20 over the probability of depositing clusters of size 10. For comparison, we reproduce the results of Fig. 2, rods all of the same size $N = 10$, curve for $\rho = 0$. The curve for $\rho = 0.5$ corresponds to the deposition of a cluster mixture having 50% of rods with size $N = 10$ and 50% of rods with size $N = 20$. A first analysis shows that the crossover appears at $l_c \approx 18$, which indicates a strong influence of large rods. However, a more careful examination of Fig. 3 shows that there are two defined slopes for $l \leq 20$ and that $l_c \approx 20$ for any value of ρ . It was found that for $l \leq 10$, the slope is $\chi_1 = 0.5$, as for $\rho = 0$, while in the range $10 \leq l \leq 20$, the HHCF adopts a smaller slope that directly depends on ρ . This is apparent in the left inset of Fig. 3 showing the HHCF normalized to the same final value in the range (10, 20) for three different mixtures of rods of sizes 10 and 20. In the right inset, the value of the slope in the range $10 \leq l \leq 20$ as a function of the mixture parameter ρ is presented.

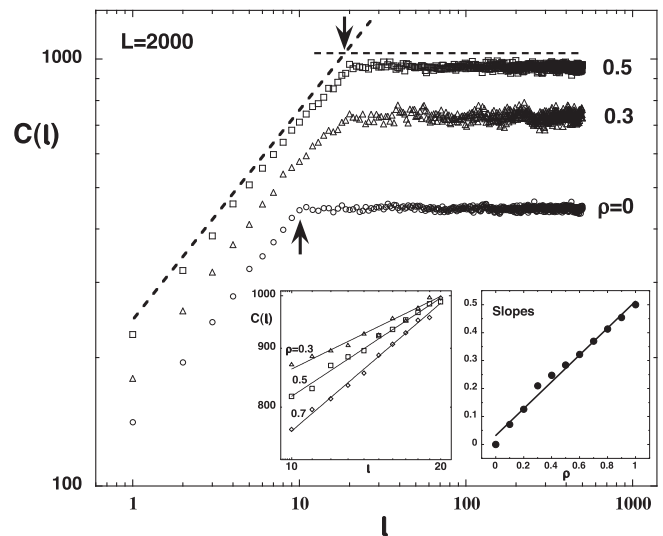


Fig. 3. Height–height correlation function for the WCD model after the deposition of a mixture of rods of size 10 and 20 for three values of ρ , the ratio between the probability of depositing clusters of size 20 over the probability of depositing clusters of size 10. An effective crossover of 18 can be determined for $\rho = 0.5$. The left inset shows that, in fact, there are two defined slopes for $l \leq 20$ and that $l_c \approx 20$ for any value of ρ . The right inset shows the value of the slope in the range $10 \leq l \leq 20$ as a function of the mixture parameter ρ .

We also studied for the WCD model the effects of depositing rods of different size. Fig. 4 shows the HHCF after the deposition of clusters with an exponential size distribution and average size equals to 10. Interestingly, the effective crossover adopts a value of about 15, higher than that corresponding to the average cluster size of $N = 10$ (curve labeled Rods 1). This indicates that the presence of large clusters, despite their shorter number, clearly affects the crossover.

Fig. 4 also shows the HHCF after the deposition of square clusters with an exponential size distribution. It can be thought that the only difference in using clusters of size $N \times N$ instead of rods is a factor N in the height of the aggregate, so nothing different than an N scale factor in $W(L,t)$ could be expected. However, the value of the crossover is about 28, much larger than that corresponding to the deposition of rods. Note that the deposition of a cluster of size $N \times N$ is equivalent to the deposition of N rods of size N . This could be equivalent to the deposition of rods with a size distribution of the form $x \cdot \exp(-x/x_0)$, where $x_0 = 10$. To check if this is the reason for the observed value of the crossover, we deposit rods using this size distribution. The curve labeled Rods 2 is the corresponding HHCF. Interestingly, the value of the resulting crossover is about 21. It is higher than that for the exponential distribution size (Rods 1) but smaller than that corresponding to the square deposition. This indicates that the simultaneous rod deposition involved in square deposition has a measurable effect. Note that the deposition of a cluster of size N is equivalent to the deposition of N rods at the same place.

In Fig. 5, we present the temporal evolution of the surface roughness $W(t)$ for a random deposition of rods of $N = 10$, averaged over 100 samples, and different system sizes ranging from $L = 130$ up to 4000 for the RCD model. The results of the simulations show that the roughness evolves in time following two different regimes and then it reaches the saturation value. At earlier times the growth exponent takes a value $\beta_1 = 0.51$ that is very close to a random deposition model, for which $\beta = 1/2$ as correlation is absent. At intermediate times, the growth exponent takes a value $\beta_2 = 0.27$ close to $\beta = 1/3$, expected for a ballistic deposition (BD) corresponding to the KPZ universality class. This is expected because, in contrast to particle random deposition that is uncorrelated, every cluster occupies several lattice sites and then correlation between neighboring columns emerges. The value of the roughness exponent obtained from the saturation values of the interface width is $\alpha_{\text{global}} = 0.41$. This value is different from $\alpha_{\text{global}} = 1/2$

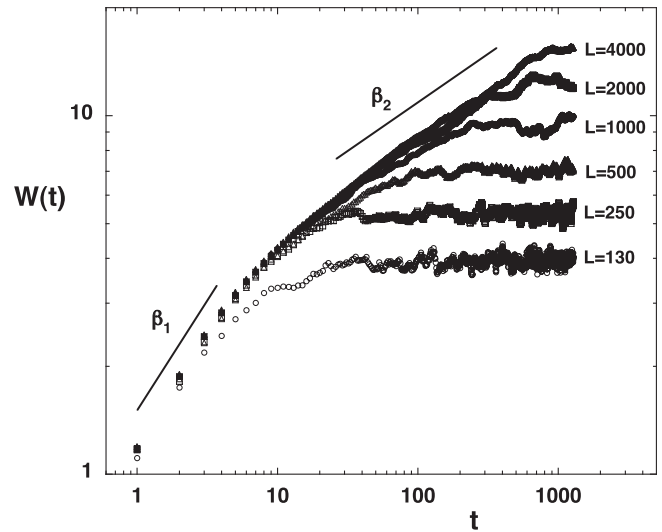


Fig. 5. Temporal evolution of the surface roughness $W(t)$, for a random deposition of 1×10 clusters and different system sizes ranging from $L = 130$ up to 4000. As can be seen, there are two regimes before saturation cause by system finite size, one for short times where $\beta_1 = 0.51$ corresponding to random deposition, and a second $\beta_2 = 0.28$.

that corresponds to the KPZ universality class, and also lower than the value reported in Ref. 8 ($\alpha_{\text{global}} \approx 0.45$), as determined from the reported results.

Fig. 6 shows the height–height correlation function for 1×10 cluster deposition as a function of the correlation distance l for different substrate sizes. Not a very large substrate is needed to clearly observe two regimes with slopes tending to 0.5 and 0.35, as dashed lines indicate. As also observed in the WCD model, the crossover length directly reflects the clusters size, $l_c \sim 10$. [16] We also checked the effects of depositing clusters of different sizes on the scaling exponents. The inset of Fig. 6 shows the local width (LW) for different rods size distributions: (a) all of size 10, (b) Gaussian distribution with standard deviation equals 4, and (c) exponential distribution. In all cases the average rod size equals 10. Two different roughness exponents are clearly detected: α_1 , at short scale (below the cluster size), and α_2 , at long scale that is

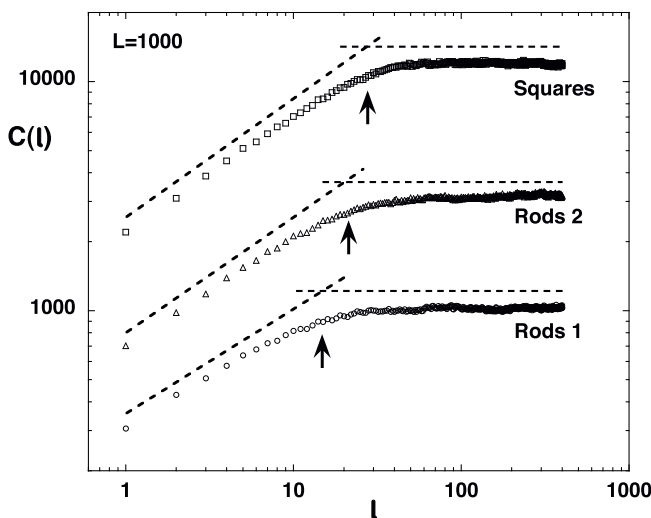


Fig. 4. Height–height correlation function for the WCD model after the deposition of rods and squares. Rods 1 refers to the deposition of rods with an exponential size distribution having an average size $x_0 = 10$. Rods 2 refers to the deposition of rods with a size distribution of the form $x \cdot \exp(-x/x_0)$. Squares refers to the deposition of squares with an exponential size distribution and average side equals to 10. Arrows indicate different crossovers for the three depositions.

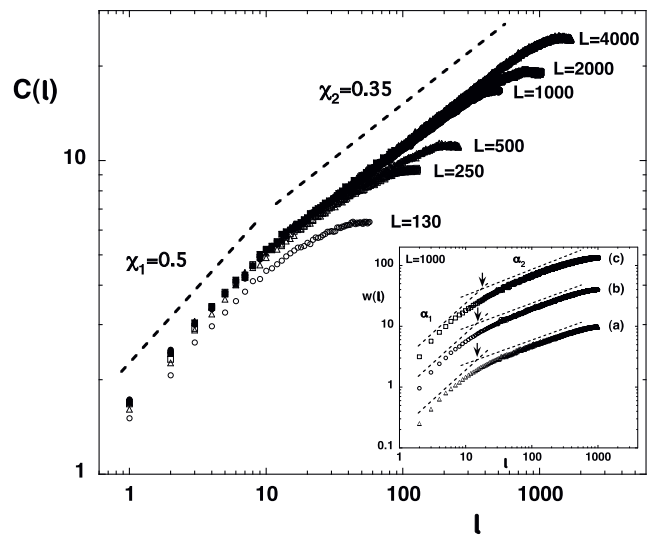


Fig. 6. Height–height correlation function for 1×10 cluster deposition as a function of the correlation distance l for different substrate sizes. Note that the crossover length directly reflects the clusters size. The inset shows the local width for different rod size distributions: (a) all rods are of size 10, (b) Gaussian distribution with standard deviation equals 4, and (c) exponential distribution. In all cases, the average rod size equals 10, $L = 1000$ after a deposition of 1000 ML.

identified with the growing dynamics. $\alpha_1 \approx 1$ for the three cases, while $\alpha_2 \approx 0.39, 0.41,$ and 0.43 for cases a, b, and c, respectively. The crossovers show similar sensitivity to rod size distributions as in the WCD model. We can determine that $l_C \sim 15$ for cases a and b and $l_C \sim 18$ for case (c). The analysis for the HHCF shows the same trends, but it is more difficult to determine the crossovers due to the close values of χ_1 and χ_2 . However, as pointed out above, the local crossover points for the HHCF match the size of the deposited clusters, whereas the LW tends to overestimate it [17].

The spectral power density or structure factor for different substrate lengths for 1×10 rods are presented in Fig. 7. Two slopes can be extracted, from low and high valued of k . The slope for large k 's does not vary much as a function substrate length and an average value of 0.42 is determined, consistent with the value of α_{global} obtained from the roughness saturation values. Conversely, for low k 's, α_2 monotonically increases with the substrate length matching the trend shown in the height–height correlation function, with a value of 0.33 extracted from results corresponding to $L = 4000$.

The cluster size influence on the short and long range of the HHCF and the LW was studied after the deposition of clusters of different sizes. Fig. 8 shows the influence of the cluster size on the roughness exponent obtained from the LW for rods with sizes $N = 2, 10, 20,$ and 40 . It is observed that the total roughness decreases with N since the surface tends to flatten as the rod size increase. The roughness exponent α_1 is about 0.64 for $N = 2$ to rapidly converge to $\alpha_1 \approx 1$ for $N \geq 10$. On the other hand, the exponent roughness α_2 does not show any dependence on the cluster size.

In Fig. 9, we plot the values for the large-scale roughness exponents obtained from the LW (α_2) and from the HHCF (χ_2) as well as the large-scale growth exponent β_2 obtained from the roughness evolution for a cluster size of 1×10 . Both α_2 and χ_2 seem to tend to a common value below 0.4, slightly smaller than the α_{global} determined from the saturation roughness $W(L,t)$ shown in Fig. 4. This value is far from $\alpha_{\text{global}} = 1/2$ expected for KPZ universality class in 1D [22].

The KPZ equation was long ago proposed as the continuous counterpart of ballistic deposition. However, numerical simulation failed systematically in finding a clear connection between them. Indeed, scaling exponents for BD have been regularly found smaller than those corresponding to KPZ. The agreement was achieved using enormously large-scale simulations [23]. Previously, strong finite-size corrections were considered responsible for the discrepancies and then the use of effective exponents was recommended [24]. More recently, scaling exponents for BD were brought into agreement with the KPZ

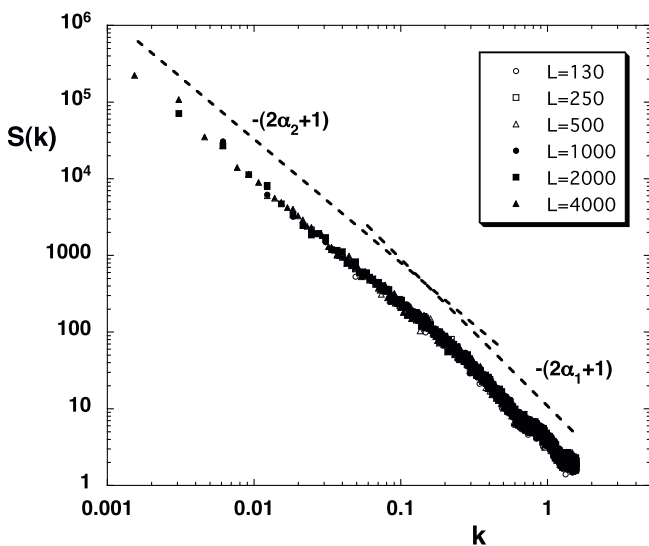


Fig. 7. Spectral power density or structure factor for different substrate lengths. Values for α_1 and α_2 can be extracted.

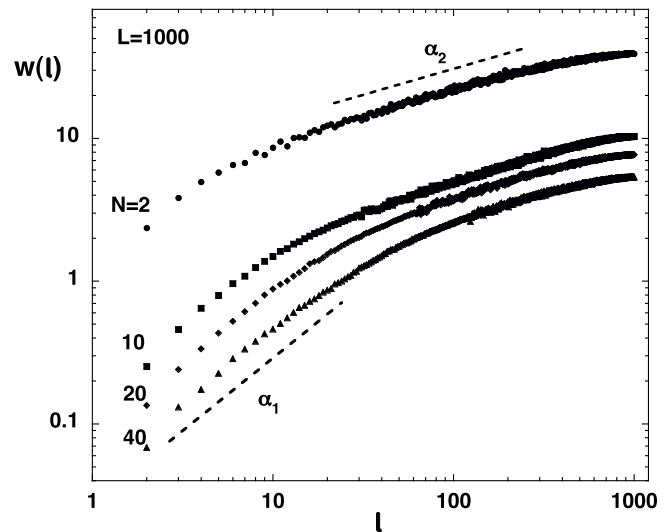


Fig. 8. Local widths for the RCD model with rods of sizes $N = 2, 10, 20,$ and 40 . As expected, the roughness decreases and the crossover moves to higher values of l as rods are larger. Also, as N increases, α_1 can be determined more accurately, and we found that it tends to 1. On the contrary, it is easier to determine α_2 for smaller values of N . For $N = 2$, $\alpha_2 = 0.37$.

class by tracing down corrections to fluctuations in the height increments along deposition events with resulting surfaces having narrow and deep valleys [25].

Surface heights after cluster deposition are similarly correlated as in BD due to the inherent lateral growth present in both mechanisms. Then, we expect that the exponents for the RCD model should converge to those corresponding to the KPZ universality class. In Ref. [25], the authors proposed a method to suppress corrections consisting in dividing the surface in bins and then using the maximal height inside each bin to do the statistics. We found that for small clusters of size 2, the surface presents deep valleys that are eliminated with this method and the exponents become much closer to those of KPZ. Interestingly, surfaces after the deposition of clusters of size 10 do not show such valleys, and we found that the proposed method produces no effect on the determined scaling exponents.

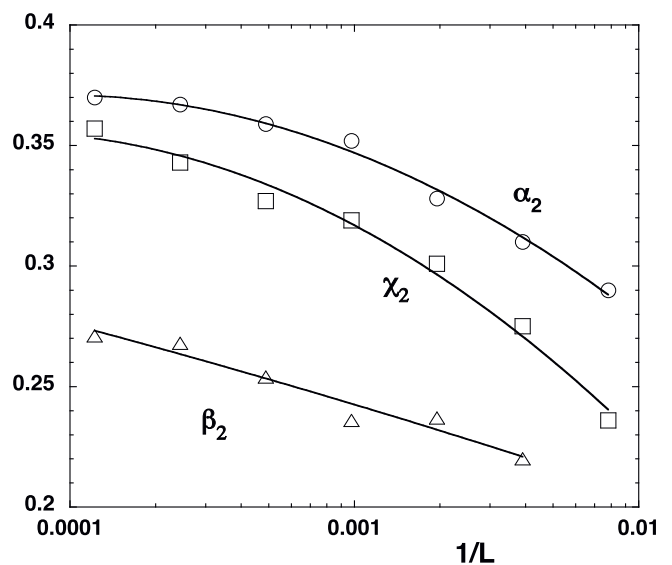


Fig. 9. Values of the intermediate regime scaling exponents as a function of the system size L . Growth exponent β_2 and roughness obtained from W , and α_2 and χ_2 obtained from LW and HHCF, respectively. We found that the exponents are affected by finite-size effects as they should converge to BD exponents ($\beta = 0.33, \alpha = 0.5$).

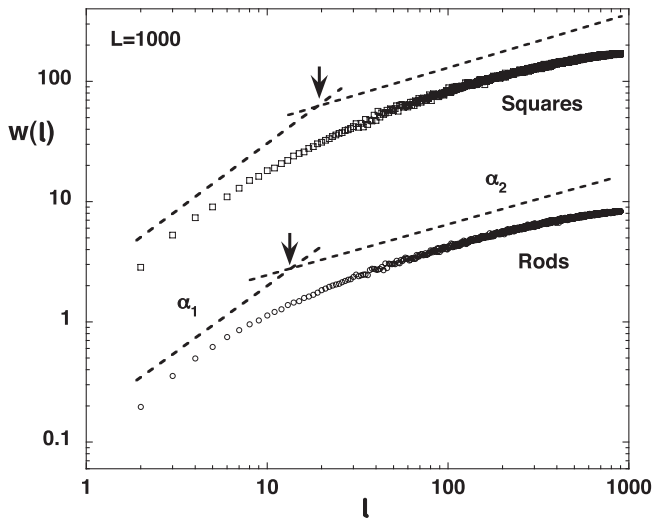


Fig. 10. Local widths for the RCD model after the deposition of 1000 ML of rods and squares for $L = 1000$. The clusters size distribution is exponential with average size equals 10 for both cases. Note that the local width corresponding to square clusters is not simply the corresponding to rods multiplied by a factor.

Finally, we studied, for the RCD model, the difference between rods and squares clusters deposition. We found that when squares of size $N \times N$ and rods of size $1 \times N$ are deposited, the absolute value of the roughness, as expected, is N times larger since each time a cluster of size $N \times N$ is deposited the surface height locally increases N times respect to the deposition of a $1 \times N$ cluster. However, this is not the case when clusters of different sizes are deposited. For example, as shown in Fig. 10, for an exponential cluster size distribution of mean size 10, the roughness do not simply differ by a factor of 10. In fact, different values for the roughness exponents results slightly different α_2 , 0.42 for rods and 0.46 for squares, and the crossovers $l_c \approx 14$ for rods and 20 for squares. The reason for this can be those discussed for the WCD model. Also, for the RCD model, the aggregation of squares of different sizes leads to structures that not only differ by a factor in the height respect to the aggregation of rods, and this also can be responsible for the above findings.

5. Conclusions

Using the Monte Carlo simulations in 1D, we studied two surface growth models with random deposition of clusters using two types of aggregation mechanisms: one in which clusters wet the surface copying its profile (WCD), and other using rigid clusters that stick at the first point of contact and do not change their shape (RCD). Depending on the type of deposition mechanism imposed, the system exhibits

different scaling. In the wetting cluster deposition model, the system exhibits the usual random deposition exponents for large window sizes, but a correlation appear for windows up to about the cluster size. We found that the crossover length is affected by the cluster size and also by the cluster size distribution, while the local roughness exponents are only affected by the substrate finite size. The rigid cluster deposition model behaves as a BD process due to lateral correlations introduced through the finite size of the clusters. Results for the RCD model show two different behaviors in time before the saturation value is reached. Initially growing is uncorrelated, then roughness increases with a smaller exponent to finally reach saturation. In space, two different roughness exponents are detected, at scales below and above the cluster size. By analyzing systems of different sizes using various indicators it can be found that the model slowly converges to the KPZ universality class.

Acknowledgments

This work was supported by the National Council for Scientific and Technical Research of Argentina (CONICET) and the University of Mar del Plata (Argentina).

References

- [1] See, for example, Charles B. Duke, E. Ward Plummer, *Frontiers in Surface and Interface Science*, Elsevier, Amsterdam, 2002.
- [2] A.-L. Barabási, H.E. Stanley, *Fractal Concepts in Surface Growth*, Cambridge University Press, Cambridge, 1995.
- [3] F. Family, T. Vicsek, *J. Phys. A* 18 (1985) L75.
- [4] F. Family, T. Vicsek, *Dynamics of Fractal Surfaces*, World Scientific, Singapore, 1991.
- [5] A. Chame, F.D.A. Arao Reis, *Surf. Sci.* 553 (2004) 145.
- [6] K. Nielsch, R.B. Wehrspohn, J. Barthel, J. Kirschner, U. Gsele, S.F. Fischer, H. Kronmüller, *Appl. Phys. Lett.* 79 (2001) 1360.
- [7] R. Karmhag, T. Tesfamichael, E. Wackelgard, G.A. Niklasson, M. Nygren, *Sol. Energy* 68 (2000) 329.
- [8] Zh. Ebrahiminejad, S.F. Masoudi, R.S. Dariani, S.S. Jahromi, *J. Chem. Phys.* 137 (2012) 154703.
- [9] F.L. Forgerini, W. Figueiredo, *Phys. Rev. E* 79 (2009) 041602.
- [10] F.L. Forgerini, W. Figueiredo, *Phys. Rev. E* 81 (2010) 051603.
- [11] J.B. Chen, J.F. Zhou, A. Häfele, C.R. Yin, W. Kronmüller, M. Han, H. Haberland, *Eur. Phys. J. D* 34 (2005) 251.
- [12] H. Haberland, Z. Insepov, M. Moseler, *Phys. Rev. B* 51 (1995) 11061.
- [13] J.W. Kang, K.S. Choi, J.C. Kang, E.S. Kang, K.R. Byun, H.J. Hwang, *J. Vac. Sci. Technol. A* 19 (2001) 1902.
- [14] J.W. Kang, H.J. Hwang, *Comput. Mater. Sci.* 23 (2002) 105.
- [15] T.J. Oliveira, F.D.A. Arao Reis, *J. Appl. Phys.* 101 (2007) 063507.
- [16] T.J. Oliveira, F.D.A. Arao Reis, *Phys. Rev. E* 83 (2011) 041608.
- [17] D.A. Mirabella, C.M. Aldao, *Phys. A* 45 (2013) 0234.
- [18] J.M. Lopez, *Phys. Rev. Lett.* 83 (1999) 4594.
- [19] J.J. Ramasco, J.M. López, M.A. Rodríguez, *Phys. Rev. Lett.* 84 (2000) 2199.
- [20] W. Schwarzacher, *J. Phys. Condens. Matter* 16 (2004) R859.
- [21] H. Xia, G. Tang, Z. Xun, D. Hao, *Surf. Sci.* 607 (2013) 138.
- [22] R. Miranda, M. Ramos, A. Cadilhe, *Comput. Mater. Sci.* 27 (2003) 224.
- [23] B. Farnudi, D.D. Vvedensky, *Phys. Rev. E* 83 (2011) 020103.
- [24] F.D.A. Arao Reis, *Phys. Rev. E* 63 (2001) 056116.
- [25] S.G. Alves, T.J. Oliveira, S.C. Ferreira, *Phys. Rev. E* 90 (2014) 052405.